Journal of
Ceramic Science
and Technology

J. Ceram. Sci. Tech., 07 [04] 357-364 (2016)
DOI: 10.4416/JCST2016-00045
available online at: http://www.ceramic-science.com

Microstructure and Electrical Properties of Co-Doped ZnO Varistors

S. Hamdelou[1], K. Guergouri[*1, 2]

[1]Laboratoire de Physique-chimie des Semiconducteurs, Université des Frères Mentouri-Constantine, Constantine 25000 Algeria.
[2]Département de Physique, Faculté des Sciences Exactes et des Sciences de la Nature et de la Vie, Université d'Oum El Bouaghi, 04000, Algeria.

received April 16, 2016; received in revised form August 17, 2016; accepted September 23, 2016

Abstract

Varistor ceramics based on Co-doped ZnO nanopowders were prepared with the sol-gel method. The analysis of the structure shows that the ZnO:Co (1 mol%, 3 mol%, 5 mol% and 7 mol%) has a wurtzite structure without any second phase, the Co ions successfully substitute Zn sites in the ZnO lattice. The grain size of the obtained nanopowders varies between 36 and 210 nm. The microstructure and electrical properties of varistors made of these powders have been studied as a function of the sintering temperature, which ranged between 900 °C and 1075 °C. The varistors were sintered by means of the microwave method. The results obtained show that the grain size of the ZnO nanopowders decreases with increasing Co content, and increases with rising of the sintering temperature, the threshold voltage increases with decreasing grain size with values varying between 99 V/mm and 681.3 V/mm.

Typically, the varistor ceramics with 5 mol% Co sintered at 1000 °C exhibit the best electrical properties with a threshold voltage of 333.5 V/mm and a nonlinear coefficient of 15.32. The results also show that doping with Co atoms is a promising route to obtaining a higher threshold voltage of varistor ceramics based on ZnO nanopowders.

Keywords: Co-doped ZnO varistors, microwave sintering, microstructure, electrical properties

I. Introduction

ZnO varistors are well known for their highly nonlinear current-voltage characteristic with a highly resistive state in the pre-breakdown region and their large non-linearity coefficient [1]. This was the reason why the varistors have been used extensively for the protection of electronic circuits, devices and equipment against voltage surges, and for the voltage stabilization of electrical power lines, for almost 30 years. The characteristics of varistor ceramics are closely related to their microstructure, which is characterized by: the grain size and distribution, the grain boundaries, the secondary phases and their distribution along the grain boundaries, and the presence or not of porosity. Up until now, the majority of commercial ZnO varistor materials have been semiconductor Bi-doped ZnO [2], because of their limited drawbacks owing to the high volatility and reactivity of the liquid phase of Bi_2O_3 during the sintering [3]. However, several studies have been conducted involving the addition of other oxides such as Pr_6O_{11}, CoO, La_2O_3, Sb_2O_3, Cr_2O_3, Dy_2O_3, MnO_2 [3,4,5,6]. To manufacture high-performance varistor ceramics, good homogeneity of the starting oxide mixture is needed. Conventional varistors are usually prepared by mixing 0.2 – 1 µm-sized ZnO powders with oxide additives. The grain size of the obtained products is in the range of 5 – 12 µm and the corresponding breakdown voltage (E_b) is around 200 – 400 V/mm for conventional varistors [7]. In several experiments, it was observed that the grain sizes and the characteristics of the grain boundaries within the same ZnO varistor causes a decrease or an increase of the breakdown voltage values [8,9,10]. In previous work, for CO-Zn binary varistor, it was found that the decrease in grain size, resulting in an increase of E_b, improves the coefficient α [11]. The homogeneity of the starting oxide mixture is therefore important to manufacture high-performance ceramic varistors. Thus the advantages of a better chemical homogeneity, higher powder purity, and a more uniform grain size can be decisive in the use of these varistors if the final electrical properties are greatly improved [12].

Varistors made from powders with small grains can be sintered at temperatures below those required for varistors with larger grains. [13,14]. To obtain optimal powder, the sol-gel method has been used [12]. The microwave sintering method is considered to be effective in obtaining high density samples [11], but the electrical features are not remarkable yet [15]. Subasri *et al.* showed that microwave-sintered samples exhibit finer grain size and higher density than those obtained by conventionally sintered samples, with similar temperature profiles [16]. Some articles report that the cobalt is very important to improve electrical characteristics of ZnO varistors [17,18,19]. Some references [19,20,21] indicate that CoO-doped ZnO varistors have mostly focused on commercially available micron-sized starting powders and conventional sintering, hence, the present study investigated microwave sintering of nanocrystalline doped ZnO powders. In addition, in this work we tried to understand the effect of Co concentration and the sintering temperature on the microstructure and electrical properties of ZnO-CoO binary varistors.

* Corresponding author: kamelguergouri@yahoo.com

II. Experimental Procedure

Co-doped ZnO nanopowders in the range of 0–7 mol% were synthesized with the sol-gel method.

The reagents used are zinc acetate dehydrate [Zn $(CH_3COO)_2 \cdot 2H_2O$, purity: 99 %, Biochem-Chempharma)], cobalt acetate tetra hydrate [$Co(CH_3COO)_2 \cdot 4H_2O$, purity: 99 %, Biochem-Chempharma], lactic acid and ethanol.

First, the zinc acetate dehydrate and cobalt acetate tetrahydrate are dissolved in ethanol, and then the obtained solution is stirred at 70 °C for 2 h. The following step consisted in dripping lactic acid into the obtained mixture until a transparent and homogeneous solution was obtained.

The molar ratio of ethanol to lactic acid is 3. The final solution was then dried at 100 °C for 1 h and calcined in air at 550 °C for 2 h. At the end, a kind of a green nanopowder is obtained.

The obtained nanopowders were pressed by disks with diameter of 12 mm under 75 MPa pressure. Then they are sintered in a microwave furnace (model 2.45 GHz, 850 W) at different temperatures, 900 °C, 1000 °C, 1050 °C and 1075 °C for 15 minutes. In previous work [11], we demonstrated that the use of the microwave sintering process allowed us to manufacture varistors with good quality (low density and efficient electrical properties).

The structure of the nanopowders was identified by means of XRD using the Cuk_α radiation of a BRUKER AXS, D8 advance X-ray diffractometer. The peaks of the spectrum permit us to calculate the average of the particle size of the powders using Scherrer's equation [22]:

$$d = \frac{0.9\lambda}{\Delta\theta \mathrm{Cos}\theta} \qquad (1)$$

where d is the particle size, λ the x-ray wavelength (λ = 1.5418A°), **Δθ** the full width at half-maximum (FWHM) and θ the Bragg angle. The density of the sintered samples is measured by means of Archimedes' method using a SCALTEC SBC22 analytical weighing balance and the microstructure and morphology of ceramics are observed with a VEGA TS 5,130 MM, TESCAN Scanning Electron Microscope (SEM).

The average particle size (D) of the sintered samples is determined with the lineal intercept method, given by the following equation:

$$D = 1.56\ L/M \qquad (2)$$

Where L is the random line length on the micrograph, M the magnification of the micrograph and N the number of grain boundaries intercepted by the lines [23, 24].

Finally, the current-voltage I(V) characteristics are measured using a direct current power supply (1500 V, 10^{-2}A), a "Nano-Ampere meter" and a "Voltmeter". The sintered samples are covered with silver paste and heated at 600 °C for 30 min. The nonlinear exponent (α) is calculated from the empirical relation [23, 25]:

$$J = KE^{\alpha} \qquad (3)$$

Where *K* is a constant, ***J*** and ***E*** the current density and electric field, respectively. *a* is given [26] by:

$$\alpha = (\log J_2 - \log J_1)/(\log E_2 - \log E_1) \qquad (4)$$

with: J_1 = 0.1 mA, J_2 = 1 mA, E_1 and E_2 are the electric fields corresponding to J_1 and J_2, respectively

III. Results and Discussion

The XRD patterns shown in Fig. 1 correspond to nanopowder samples of 0 % to 7 % Co-doped ZnO, synthesized with the sol-gel process. The spectra exhibit peaks of the wurtzite structure, and there are no additional peaks

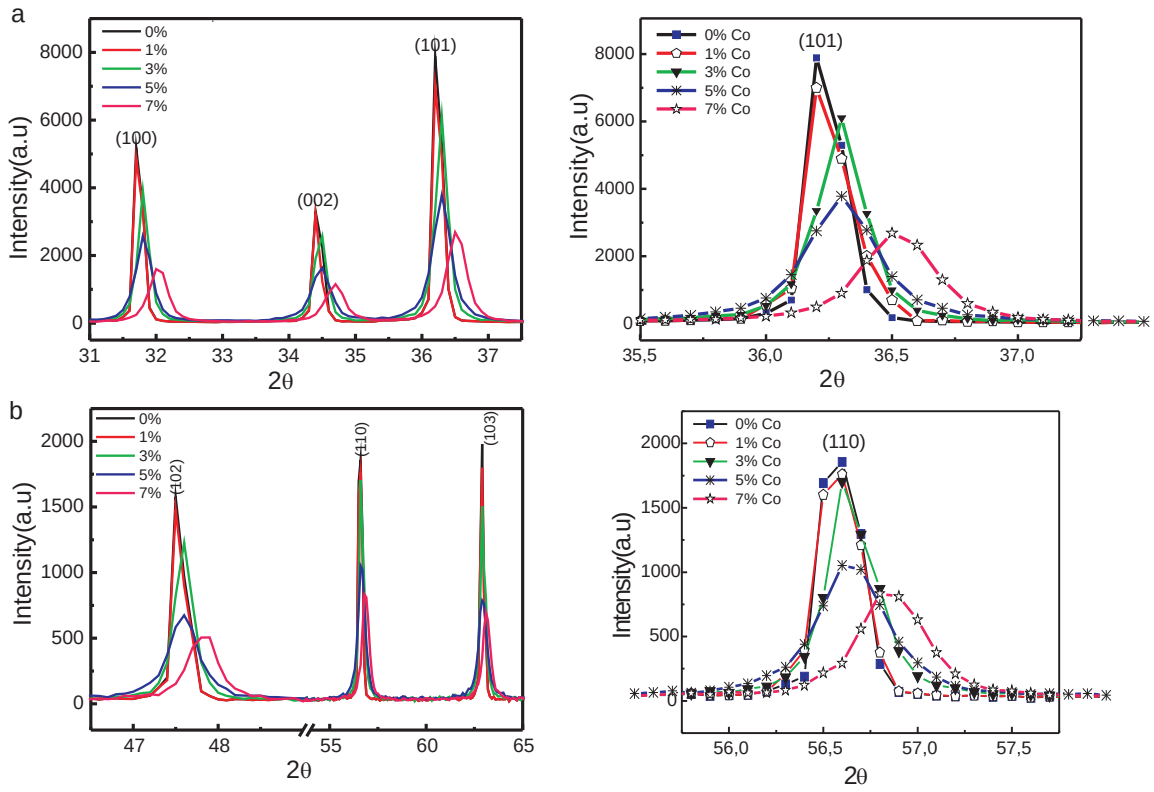

Fig. 1 a and b: XRD patterns of pure and Co-doped ZnO starting nanopowders.

after Co doping, indicating that Co is located in solid solution, which means that Co^{+2} ions are incorporated into the network based on the replacement of Zn^{+2} ions in substitutional sites. These results were confirmed by several researchers [27,28,29]. We also note that, as the concentration of Co increases, the peak intensity decreases, which can be explained in terms of degradation of the crystallinity. This means that the Co doping induces defects in the ZnO crystal. Jianping Zhou *et al.* [30] have demonstrated that these defects are located around the grains boundaries, introducing an energy barrier, thereby reducing the movement and diffusion of Zn^{+2} ions, and therefore slowing the grain growth of ZnO.

The calculation of the grain size of Co-doped ZnO nanopowders indicates that it decreases with increasing Co concentration, and it reaches its lowest value at nearly 36 nm for 7 % mol% Co as shown in Fig. 2.

Fig. 3 shows SEM images of Co-doped ZnO varistors for different Co concentrations sintered at 1075 °C, and Fig. 4 shows typical images of varistor ceramics sintered at different temperatures with different Co concentrations. All the images exhibit nanometer grain size structures with, however, some differences related to the particle size (**D**) of the starting powders, the average value of which decreases from 10 μm to 1.75 μm when the amount of Co increases.

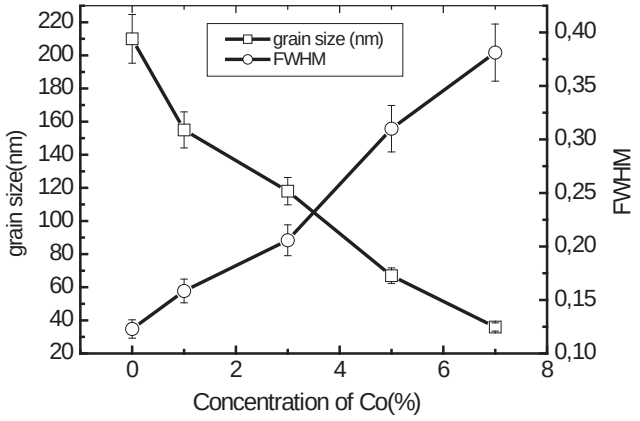

Fig. 2: FWHM (Full Width at Half-Maximum) and grain size variations of ZnO nanopowders as a function of the Co concentration.

Furthermore the SEM images show grains uniformly distributed in the presence of pores. The porosity of pure ZnO is very small, but for the doped samples it becomes more important, it decreases when the Co content increases, it is between 10 % for 1 % Co to 3.88 % for 7 % Co. Thus, one can conclude that the porosity decreases with decreasing particle size of the starting powders. From Fig. 4 we noted the following average particle size: 1.05 μm for the sample of 1 % Co sintered at 1000 °C, 0.97 μm for 7 % Co sintered at 1000 °C and 1.12 μm and 1.65 μm for 5 % Co sintered at 1000 °C and 1050 °C respectively.

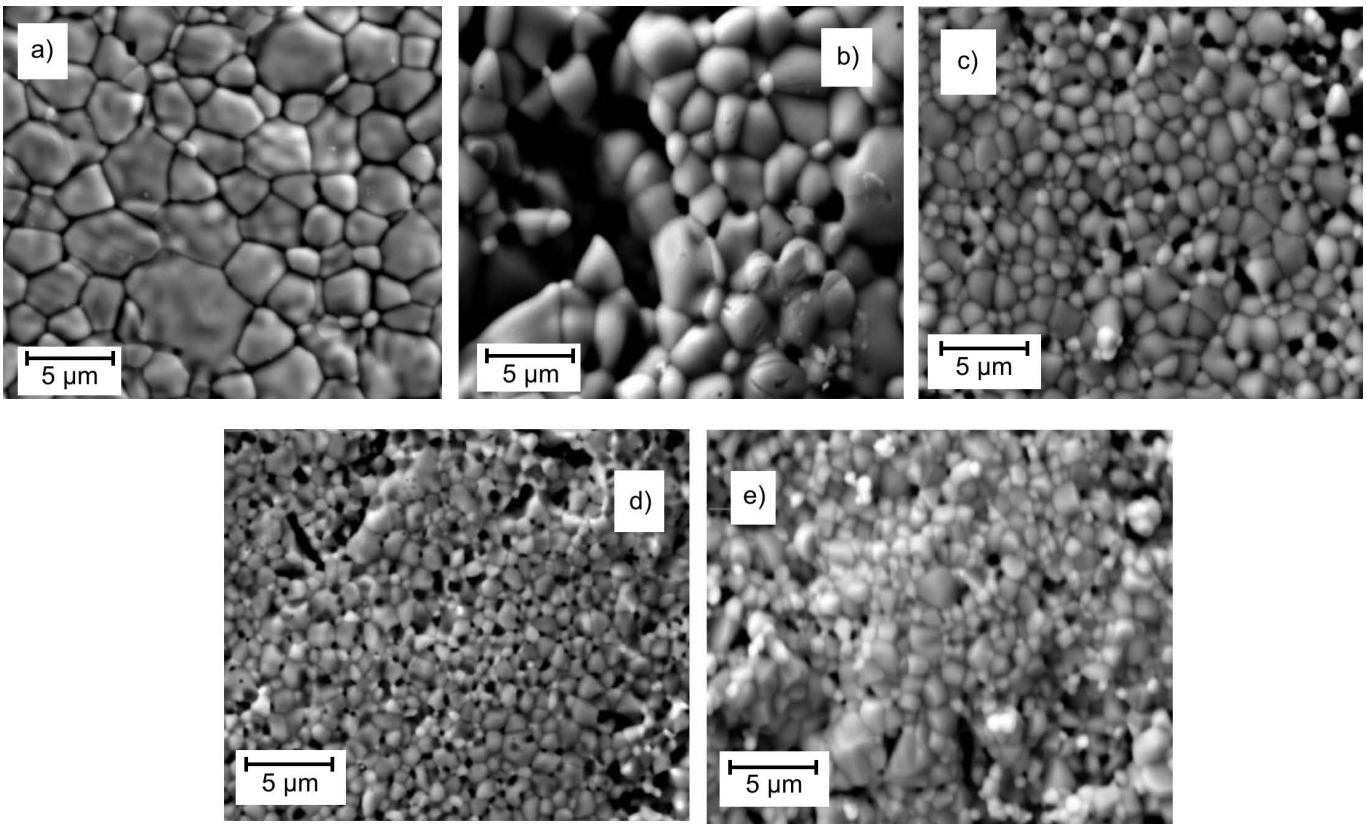

Fig. 3: SEM images of pure and Co-doped ZnO nanopowders sintered at 1075 °C: a): pure ZnO, b): 1 % Co, c): 3 % Co, d): 5 % Co, e): 7 % Co.

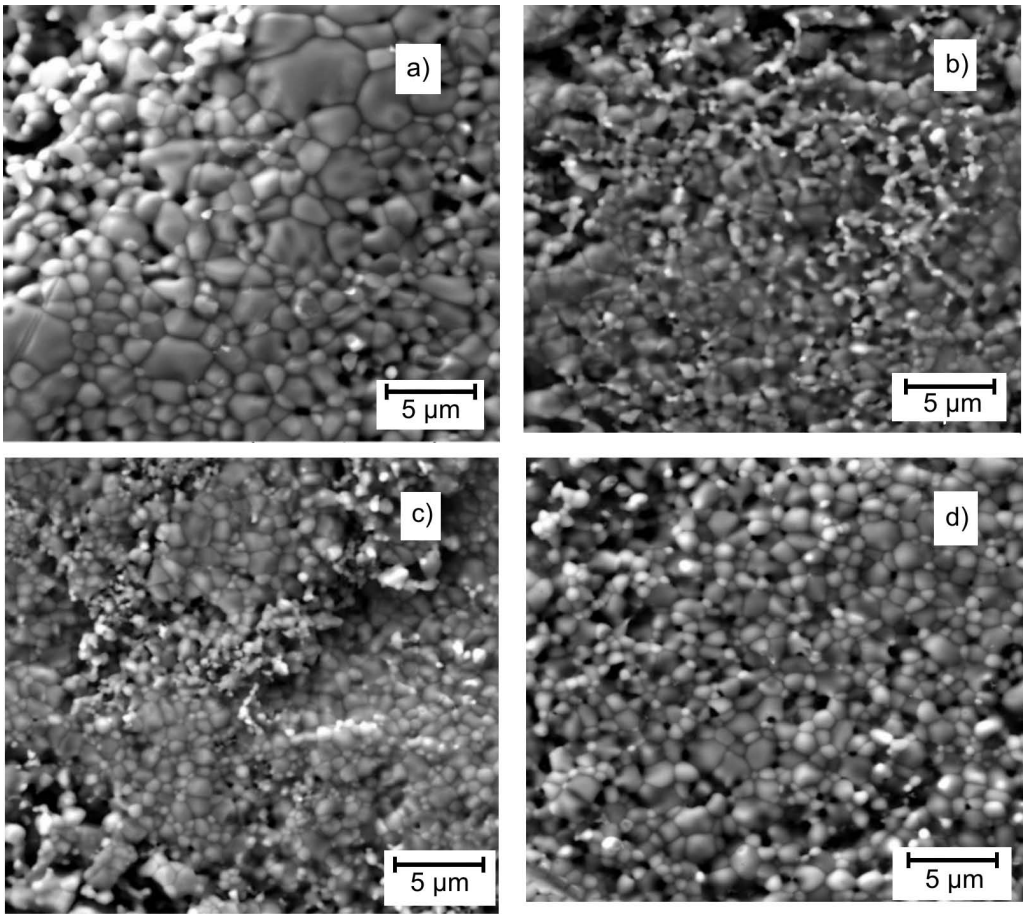

Fig. 4: SEM images of Zn-Co-O varistors: a) ZnO-1 % Co sintered at 1000 °C, b) ZnO-7 % Co sintered at 1000 °C, c): ZnO-5 % Co sintered at1000 °C, d) ZnO-5 % Co sintered at 1050 °C.

Figs. 5 and 6 show the density and the relative withdrawal of 0 %, 1 %, 3 %, 5 % and 7 % Co-doped ZnO ceramics sintered at 1075 °C. We note that the density of the pellets increases from 5.02 to 5.22 g/cm^3 with increasing Co amount. The increase of the density is due to the decrease in the grain size of starting powders, linked to the increase in the Co concentration. The same explanation can be given to the relative withdrawal, the values of which vary from 10.48 % for pure ZnO to 17.44 % for Zn-7% Co-O (Fig. 6).

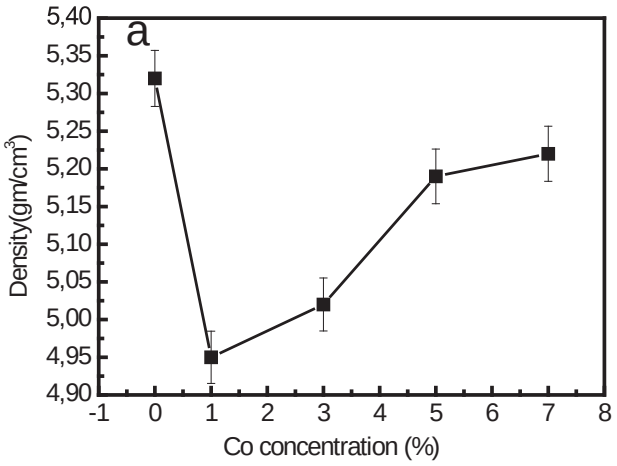

Fig. 5: Variation of the density with the Co content.

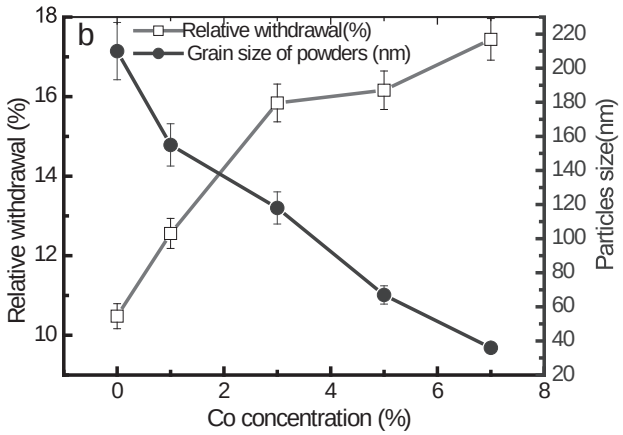

Fig. 6: Variation of the relative withdrawal with the Co content.

In Figs. 7 and 8 we plotted the density and the weight loss for different Zn-xCo-O sintered at temperatures ranging between 900 °C and 1075 °C. The results show that the density increases with increasing sintering temperature. It is important to note that the density values of the varistors with 1 % Co and 3 % Co for sintering temperatures between 900 °C and 1000 °C are lower in comparison with the values of the two others, i.e.: 5 % Co and 7 % Co.

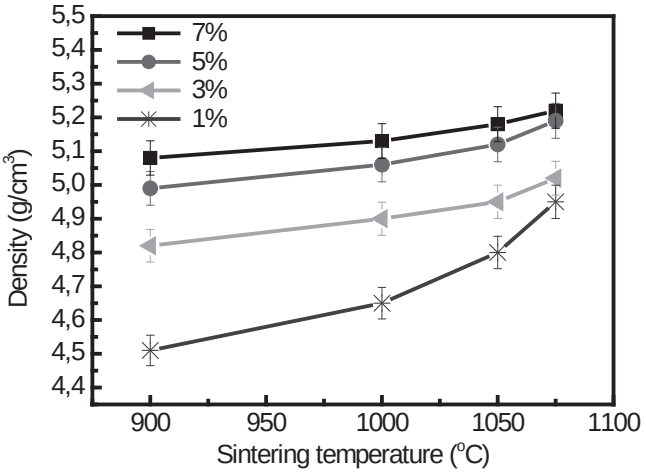

Fig. 7: Variation of the density with the sintering temperature.

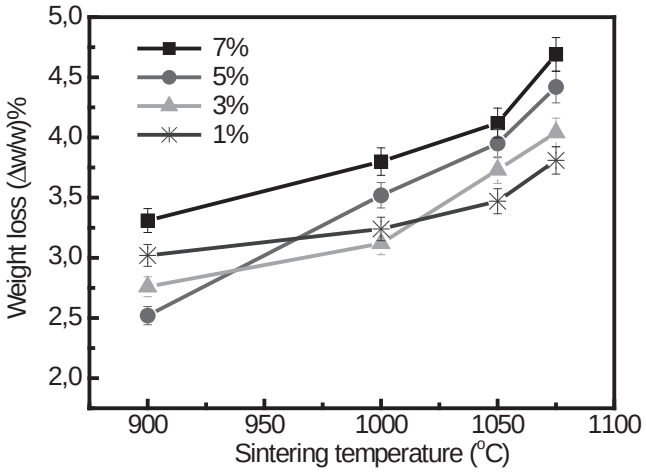

Fig. 8: Variation of the weight loss with the sintering temperature.

The weight losses of ZnO varistors sintered at temperatures in the range of 900 – 1075 °C for 15 min were plotted (Fig. 8). We observe that the weight loss evolution with temperature is almost linear. The weight loss increases, in small quantities, with sintering temperature; the values of weight loss vary between 2.5 % and 4.5 %. This is probably due to the evaporation of various elements such as water, hydrogen and carbon, and cobalt, which evaporates at high sintering temperatures, as reported by Alexander Badev *et al.* [6].

Figs. 9, 10, 11 and 12 show, respectively, the electrical characteristics E(J) of Zn-1%Co-O, Zn-3%Co-O, Zn-5%Co-O and Zn-7%Co-O specimens sintered at different temperatures, E being the electric field (V/cm) and J the current density (A/cm^2). It is clear that the breakdown curve shifts to higher electric field region with decreasing sintering temperature of all the specimens. The V_b values are higher at 900 °C (681.3 V/mm) for Zn-7 % Co-O compared to 446.5 at 1075 °C. It is also clear that the values of E_b increase with increasing Co content, as an example, we recorded the value of 128 V/mm for Zn-1 %Co-O and 561.3 V/mm for Zn-7 %Co-O at the same sintering temperature (1000 °C).

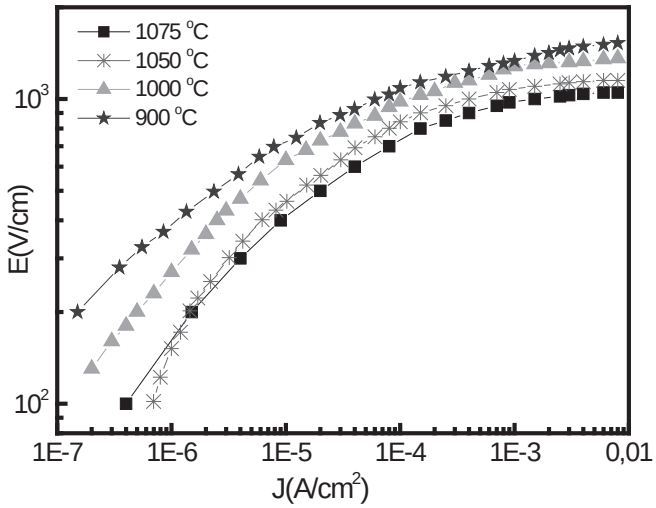

Fig. 9: Sintering temperature effect on the non-ohmic behavior of 1 %-Co-doped ZnO varistors.

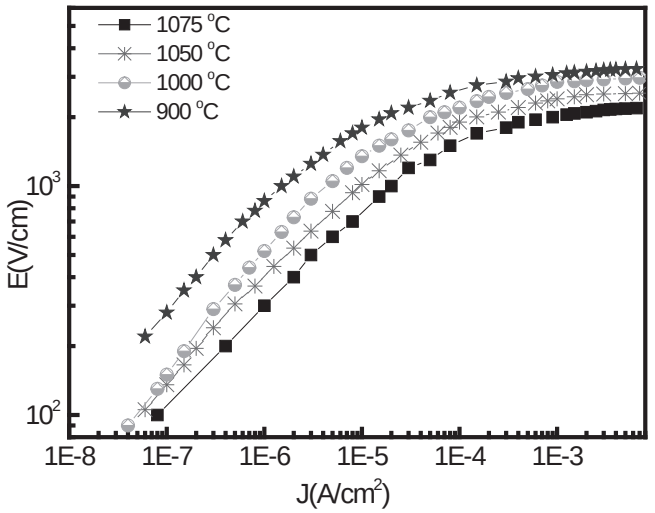

Fig. 10: Sintering temperature effect on the non-ohmic behavior of 3 %-Co-doped ZnO varistors.

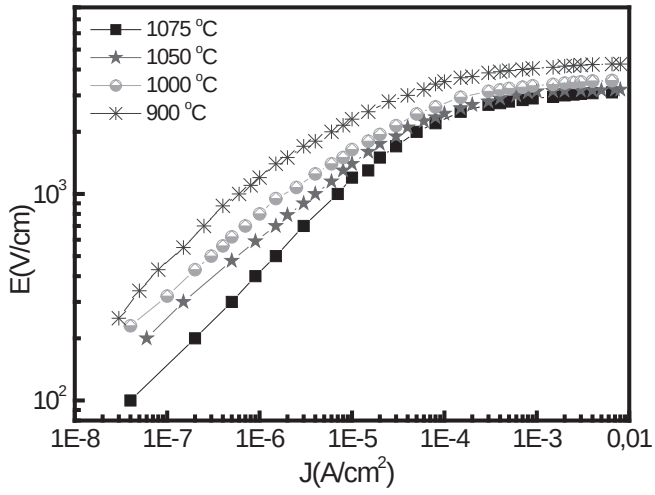

Fig. 11: Sintering temperature effect on the non-ohmic behavior of 5 %-Co-doped ZnO varistors.

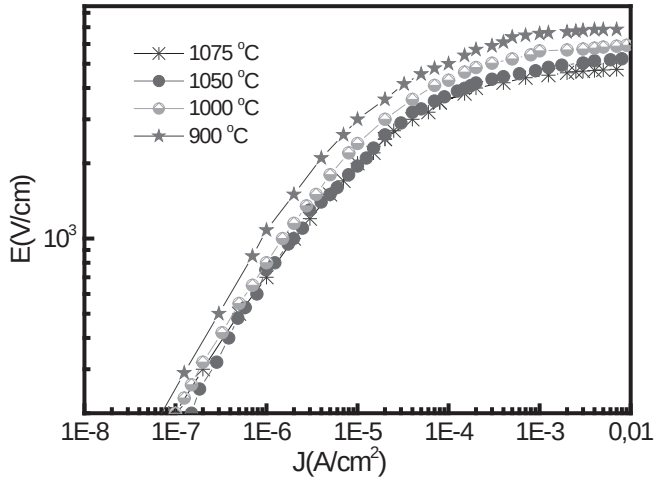

Fig. 12: Sintering temperature effect on the non-ohmic behavior of 7 %-Co-doped ZnO varistors.

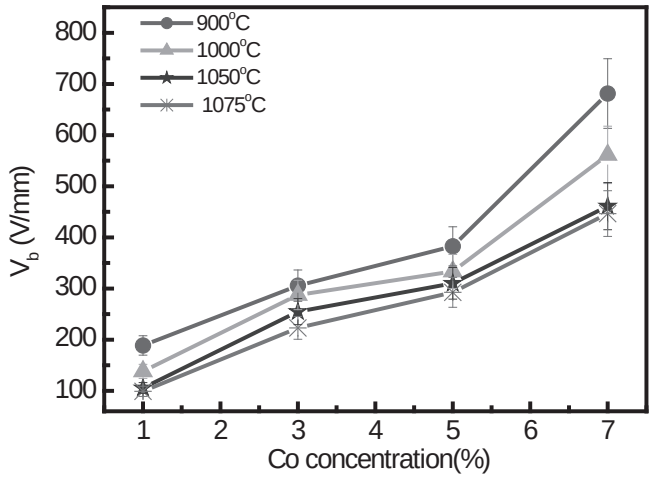

Fig. 13: Sintering temperature effect on the breakdown voltage (V_b).

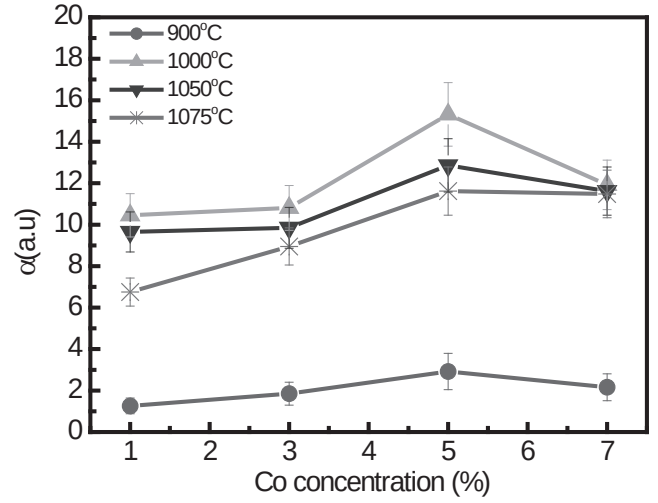

Fig. 14: Sintering temperature effect on the non-linearity coefficient α.

Variations of the breakdown voltage (V_b), the nonlinear coefficient (α), evaluated from the electrical measurements are plotted as functions of Co content and sintering temperatures as shown in Figs. 13 and 14. It has been demonstrated by Chul-Hong Kim and Guo-hua Chen [31, 32] that the breakdown voltage is related to the grain size. Fig. 13 shows that the breakdown voltage decreases with increasing grain size, which increases with increasing sintering temperature. The recorded threshold voltage V_b present values varying in a very wide range 99 – 681.3 V/mm, 681.3 V/mm is related to Zn-7 %Co-O sample sintered at 900 °C.

Fig. 14 also shows that the maximum value of α equal to 15.32 concerns the sample made with 5 mol% concentration of Co sintered at 1000 °C, which is the best sintering temperature for all samples. At 900 °C, α values vary from 1.26 to 2.92.

IV. Conclusions

A nano-sized Co-doped ZnO powder was synthesized with the sol-gel method, which is a wet chemical route. The microstructure of Co-doped ZnO varistors, sintered using the microwave method, present a homogeneous distribution of nano-metric grains in the presence of a certain porosity that decreases with increasing Co content and sintering temperature.

The breakdown voltage of the Co-doped ZnO varistors decreases with increasing grain size, which increases with increasing sintering temperature.

As regards the non-linearity coefficient, the best values were found for the sample of ZnO doped with 5 % Co and sintered at 1000 °C.

The most important result is that the reduction in the size of the powder particles leads to the decrease in the grain size of the ceramics and therefore allows the use of a low sintering temperature.

References

1 Xu, D., Cheng, X.-N., Yan, X.-H., Xu, H.-X., Shi, L.-Y.: Sintering process as relevant parameter for Bi_2O_3 vaporization from ZnO-Bi_2O_3-based varistor ceramics, *T. Nonferr. Metal Soc.*, **19**, 1526 – 1532, (2009).

2 Peng, Z., Fu, X., Zang., Y., Fu, Z., Wang, C., Qi, L., Miao, H.: Influence of Fe_2O_3 doping on microstructural and electrical properties of ZnO-Pr_6O_{11} based varistor ceramic materials, *J. Alloy Compd.*, **508**, 494 – 499, (2010).

3 Kutty., T.R.N., Ezhilvalavan, S..: The influence of B_2O_3 non-stoichiometry on the non-linear property of ZnO varistors, *Mater. Chem. Phys.*, **38**, 267 – 273, (1994).

4 Nahm, C.W.: Microstructure and varistor properties of Y_2O_3-doped ZnO-Pr_6O_{11}-CoO-Cr_2O_3-La_2O_3 ceramics, *Ceram. Int.*, **40**, 2477 – 2481, (2014).

5 Peiteado, M., Iglesias, Y., Caballero, A.C.: Sodium impurities in ZnO-Bi_2O_3-Sb_2O_3 based varistors, *Ceram. Int.*, **37**, 819 – 824, (2011).

6 Chen G, Li, J., Yang, Y., Yuan, C., Zhou, C.: Microstructure and electrical properties of Dy_2O_3-doped ZnO-Bi_2O_3 based varistor ceramics, *Mater. Res. Bull.*, **50**, 141 – 147, (2014).

7 Gupta, T.K.: Application of zinc oxide varistors, *J. Am. Ceram. Soc.*, **73**, 1817 – 1840, (1990).

8 Daneu, N., Gramc, N.N., Recnik, A., Krzmanc, M.M., Bernik, S.: Shock-sintering of low-voltage ZnO-based varistor ceramics with $Bi_4Ti_3O_{12}$ additions, *J. Eur. Ceram. Soc.*, **33**, 335 – 344, (2013).

9 Shahraki, M.M., Shojaee, S.A., Faghihi Sani, M.A., Nemati, A., Safaee, I.: Two-step sintering of ZnO varistors, *Solid State Ionics*, **190**, 99 – 105, (2011).

[10] He, J., Liu, J., Hu, J., Zeng, R., Long, W.: Non-uniform ageing behavior of individual grain boundaries in ZnO varistor ceramics, *J. Eur. Ceram. Soc.*, **31**, 1451 – 1456, (2011)

[11] Hamdelou, S., Guergouri, K., Arab, L.: The effect of the starting powders particle size on the electrical properties of sintered co doped ZnO varistors, *Appl. Nanosci.*, DOI 10.1007/s13204 – 014 – 0382 – 613, November 2014

[12] Cheng, L.-H., Zheng, L.-Y., Meng, L., Li, G.-R., Gu, Y., Zhang, F.-P., Chu, R.-Q., Xu, Z.-J.: Electrical properties of Al_2O_3-doped ZnO varistors prepared by sol-gel process for device miniaturization, *Ceram. Int.*, **38S**, 457 – 461, (2012).

[13] Pillai, S.C., Kelly, J.M., McCormack, D.E., O'Brien, P., Raghavendra, R.: The effect of processing conditions on varistors prepared from nanocrystalline ZnO, *J. Mater. Chem.*, **13**, 2586 – 2590, (2003).

[14] Pillai, S.C., Kelly, J.M., McCormack, D.E., Raghavendra, R.: Effect of step sintering on breakdown voltage of varistors prepared from nanomaterials by sol gel route, *Adv. Appl. Ceram.*, **105**, 158 – 160, (2006).

[15] Vukovic, M., Brankovic, G., Marinkovic, Stanojevic, Z., Poleti, D., Brankovic, Z.: Ultra-high breakdown field varistors prepared from individually synthesized nanoprecursors, *J. Eur. Ceram. Soc.*, **35**, 1807 – 1814, (2015).

[16] Subasri, R., Asha, M., Hembram, K., Rao, G., Rao, T.: Microwave sintering of doped nanocrystalline ZnO and characterization for varistor applications, *Mater. Chem. Phys.*, **115**, 677 – 684, (2009).

[17] Onreabroy, W., Sirikulrat, N., Brown, A.P., Hammond, C., Milne, S.J.: Properties and intergranular phase analysis of a ZnO-CoO-Bi_2O_3 varistor, *Solid State Ionics*, **177**, 411 – 420, (2006).

[18] Nahm, C.-W., Shin, B.-C., Park, J.-A., Yoo, D.-H.: Effect of CoO on nonlinear electrical properties of praseodymia-based ZnO varistors, *Mater. Lett.*, **60**, 164 – 167, (2006)

[19] Miralles, A., Cornet, A., Herms, A., Morante, J.R.: The influence of cobalt on the electrical characteristics of ZnO ceramics, *Mat. Sci. Eng. A*, **109**, 201 – 205, (1989).

[20] Arab, L., Hamdelou, S., Harouni, S., Guergouri, K., Guerbous, L.: Structural and luminescence properties of pure and Al-doped ZnO nanopowders, *Mat. Sci. Eng B.*, **177**, 902 – 907, (2012).

[21] Nahm, C.-W., Park, J.-A., Shin, B.-C., Kim, I.-S.: Electrical properties and DC-accelerated aging behavior of ZnO-Pr_6O_{11}-CoO-Cr_2O_3-Dy_2O_3-based varistor ceramics, *Ceram. Int*,, 30, 1009 – 1016, (2004).

[22] Wurst, J.C., Nelson, J.A.: Lineal intercept technique for measuring grain size in two-phase polycrystalline ceramics, *J. Am. Ceram. Soc.*, **55**, 109 – 111, (1972).

[23] Onreabroy, W., Sirikulrat, N.: Effects of cobalt doping on nonlinearity of zinc oxide, *Mat. Sci .Eng, B*, **130**, 108 – 113, (2006).

[24] Levinson, L.M., Philipp, H.R.: The physics of metal oxide varistors, *J. Appl. Phys.*, **46**, 1332, (1975)

[25] Santi, M., Laokul, P., Phokha, S.: Simple synthesis and magnetic behavior of nanocrystalline $Zn_{0.9}Co_{0.1}O$ powders by using Zn and Co acetates and polyvinyl pyrrolidone as precursors, *J. Magn. Magn. Mater.*, **305**, 381 – 387, (2006).

[26] Mesaros, A., Ghitulica, C.D., Popa, M., Mereu, R., Popa, A., Petrisor Jr.,T., Gabor, M., Cadis, A. Vasile, B.S.: Synthesis, structural and morphological characteristics, magnetic and optical properties of co doped ZnO nanoparticles, *Ceram. Int,*, **40**, 2835 – 2846, (2014).

[27] Arshad, M., Ahmed, A.S., Azam, A., Naqvi, A.H.: Exploring the dielectric behavior of co doped ZnO nanoparticles synthesized by wet chemical route using impedance spectroscopy, *J. Alloy. Compd.*, **577**, 469 – 474, (2013).

[28] Nirmala, M., Anukaliani, A.: Characterization of undoped and co doped ZnO nanoparticles synthesized by DC thermal plasma method, *Physica B*, **406**, 911 – 915, (2011).

[29] Badev, A., Marinel, S., Heuguet, R., Savary, E., Agrawal, D.: Sintering behavior and non-linear properties of ZnO varistors processed in microwave electric and magnetic fields at 2.45 GHz, *Acta. Mater.*, **61**, 7849 – 7858, (2013).

[30] Kim, C.-H., Kim, J.-H.: Microstructure and electrical properties of ZnO-ZrO_2-Bi_2O_3-M_3O_4 (M=Co, Mn) varistors, *J. Eur. Ceram. Soc.*, **24**, 2537 – 2546, (2004).

[31] Long, W., Hu, J., Liu, J., He, J.: Effects of cobalt doping on the electrical characteristics of Al-doped ZnO varistors, *Mater. Lett.*, **64**, 1081 – 1084, (2010).

[32] Lin, C.-C., Lee, W.-S., Sun, C.C., Whu, W.-H.: The influences of bismuth antimony additives and cobalt manganese dopants on the electrical properties of ZnO-based varistors, *Compos. Part B – Eng.*, 38, 338 – 344, (2007).